Generation of frustrated liquid crystal phases by mixing an achiral nematic–smectic-C mesogen with an antiferroelectric chiral smectic liquid crystal

Jan P. F. Lagerwall[a] and Frank Giesselmann
Institute of Physical Chemistry, University of Stuttgart, Pfaffenwaldring 55, D-70569 Stuttgart, Germany

Christine Selbmann, Sebastian Rauch, and Gerd Heppke
Department of Chemistry, Technical University Berlin, Berlin, Germany

(Received 3 December 2004; accepted 24 January 2005; published online 14 April 2005)

By mixing the achiral liquid crystal HOAB, exhibiting a nematic (N)–smectic-C (SmC) mesophase sequence, with the chiral antiferroelectric liquid crystal (AFLC) (*S*,*S*)-M7BBM7, forming the antiferroelectric SmC_a^* phase, at least seven different mesophases have been induced which neither component forms on its own: a twist-grain-boundary (TGB^*) phase, two or three blue phases, the untilted SmA^* phase, as well as all three chiral smectic-C-type "subphases," SmC_α^*, SmC_β^*, and SmC_γ^*. The nature of the induced phases and the transitions between them were determined by means of optical and electro-optical investigations, dielectric spectroscopy, and differential scanning calorimetry. The induced phases can to a large extent be understood as a result of frustration, TGB^* at the border between nematic and smectic, the subphases between syn and anticlinic tilted smectic organization. X ray scattering experiments reveal that the smectic layer spacing as well as the degree of smectic order is relatively constant in the whole mixture composition range in which AFLC behavior prevails, whereas both these parameters rapidly decrease as the amount of HOAB is increased to such an extent that no other smectic-C-type phase than SmC/SmC^* exists. By tailoring the composition we are able to produce liquid crystal mixtures exhibiting unusual phase sequences, e.g., with a direct isotropic-SmC_a^* transition or a temperature range of the SmC_β^* subphase of about 50 K. © *2005 American Institute of Physics*. [DOI: 10.1063/1.1872753]

I. INTRODUCTION

The family of chiral smectic-C (SmC) liquid crystal phases constitutes a fascinating set of structural variations in fluids. The combination of chirality and a layered structure in which the director **n** tilts with respect to the layer normal **k** makes all these phases locally polar, in the sense that every smectic layer carries a nonzero spontaneous polarization $\mathbf{P}_s$ in the layer plane.[1] The polarization direction can change in a complex way from layer to layer, giving the different phases varying mesoscopic polar order.[2–7] The two most important chiral smectic-C-type phases are the synclinic SmC^* and the anticlinic SmC_a^*, with parallel and antiparallel director tilt directions in adjacent layers, respectively. Since $\mathbf{P}_s$ is everywhere directed along $\mathbf{n}\times\mathbf{k}$, SmC^* becomes locally synpolar whereas SmC_a^* is antipolar. In case the helical superstructure (which renders all bulk chiral smectic-C-type phases helical antiferroelectric on a macroscopic scale[6,8,9]) is expelled by means of closely spaced substrates (surface stabilization) the SmC^* phase becomes ferroelectric,[9] hence materials exhibiting SmC^* as only chiral smectic-C-type phase are often referred to as ferroelectric liquid crystals (FLCs). If a material exhibits any other chiral smectic-C-type phase, it is usually classified as an antiferroelectric liquid crystal (AFLC). In many AFLCs the SmC_a^* phase forms on cooling from the synclinic SmC^* phase via the phases SmC_β^* and SmC_γ^*, both usually having small temperature ranges (typically 1–5 K). The last type of chiral smectic-C phase which with certainty has been identified is the SmC_α^* phase, which essentially is an extreme short-pitch version of SmC^*.[8,10,11] The present understanding of the director organizations of the five chiral smectic-C-type phases is schematically summarized in Fig. 1.

Although the properties of the different phases in the family can differ quite drastically, in particular regarding their polar nature and the dimensions and handedness of their helical superstructures, the enthalpies of the first-order transitions between these phases are extremely small, suggesting that the structural changes taking place are very subtle. The different types of correlation in tilting directions across smectic layer boundaries which distinguish the phases from each other are not yet fully understood. In particular, the SmC_α^*, SmC_β^*, and SmC_γ^* phases—often collectively referred to as the chiral smectic-C "subphases"—have been an issue of debate since they were first discovered in the AFLC compound MHPOBC.[12,13] Because the latter two appear between SmC^* and SmC_a^* in compounds exhibiting the full AFLC phase sequence, it was natural to assume that they in some way are intermediate between synclinic and anticlinic—or between ferroelectric and antiferroelectric—organization.[14–16] Since there is no simple intermediate structure between synclinicity and anticlinicity this would give the phases a frustrated character.

[a]Electronic mail: jan.lagerwall@ipc.uni-stuttgart.de

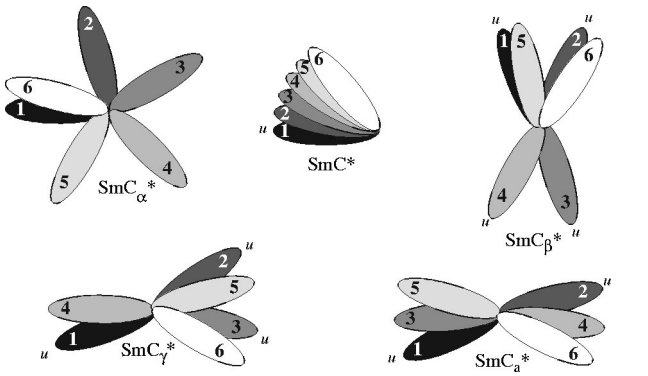

FIG. 1. Schematic overview of the director organizations in the five well-established chiral smectic-C-type phases (as they are understood today, see e.g., Ref. 7). The director tilting directions in six adjacent layers are illustrated with ellipses, the gray-shade of which illustrates the level of the layer (the layer normal is the paper plane normal): the back layer (1) is black and the front layer (6) is white. The layers constituting the smallest repeating unit (unit cell) are indicated with a *u* at the end of each ellipse. As the helical modulation superposed on the structure introduces a constant distortion between and within the repeating units, the term unit cell must be used with caution, acknowledging the fact that it is strictly meaningful only if the helical superstructure is disregarded. Since the tilt direction modulation in SmC_α^* is incommensurate with the layer spacing it is difficult to define a unit cell for this phase.

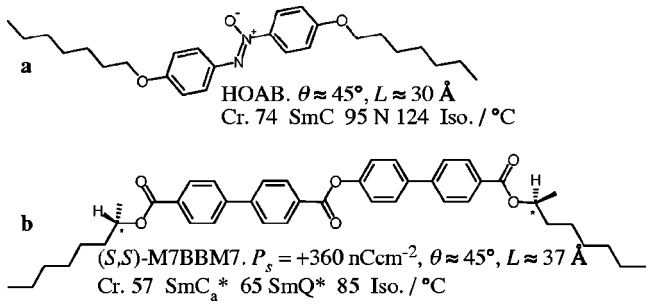

FIG. 2. Molecular constitutions of the compounds investigated.

Early on it was noticed that the subphases rapidly disappeared if small amounts of the opposite enantiomer was added to a subphase-exhibiting AFLC (Ref. 17) and somewhat later that the nonsynclinic order in AFLCs requires high degree of smectic [one-dimensional (1D) translational] order.[16,18] Recently, these two observations were developed into two different lines of reasoning regarding the requirements for the appearance of the subphases. Gorecka *et al.* proposed that the subphases are a result of strong chiral interactions and that they therefore can form only in samples of very high enantiomeric purity.[2] Lagerwall and co-workers noticed that the subphases disappeared also as a result of sample decomposition, without lowering the enantiomeric excess.[4] Based on this experimental observation and the fact that the repeating units (unit cells) of SmC_β^* and SmC_γ^* are relatively large (three and four layers, respectively, cf. Fig. 1) they proposed that the most important parameter is that of smectic order. Any substance added to an AFLC that has an adverse effect on the smectic order, whether it differs in constitution or only in the absolute configuration, could thus destabilize the subphases.

In this context, an unpublished study carried out by Bennemann *et al.* in 1995,[19] where a mixture of the achiral nematic (N)–SmC liquid crystal HOAB (Refs. 20 and 21) and the bistereogenic AFLC (*S*,*S*))-M7BBM7 (Ref. 22) (Fig. 2) was investigated, becomes highly interesting. Based on texture observations and differential scanning calorimetry (DSC), they came to the conclusion that these two liquid crystals in certain ratios produce a mixture exhibiting all three chiral smectic-C subphases, whereas these phases are absent in both components on their own. At first sight, this observation would seem to be in contradiction with both lines of reasoning, since the subphases in this system appear at reduced optical and chemical purity, i.e., where the chiral interactions as well as the smectic order can be expected to be weaker than in the AFLC compound on its own. We have now made a more thorough investigation of this system. Our conclusion is that, although the subphases require both chirality and high smectic order, they represent maxima in neither parameter. The fundamental requirement seems to be the frustration between synclinicity and anticlinicity. The studied system also exhibits induced twist-grain-boundary (TGB^*) phases—characterized by frustration between nematic and smectic organization—and blue phases (BP^*). Furthermore, it allows for a roughly tenfold extension of the subphase temperature range as compared to typical single-component AFLCs, as well as a study of the unusual direct transition from the isotropic liquid to SmC_a^*.

II. EXPERIMENT

Eighteen different mixtures of (*S*,*S*)-M7BBM7 and HOAB, with the concentration *x* of the first component varying between 0.05 and 0.8, were prepared and studied in addition to the two pure components on their own. (*S*,*S*)-M7BBM7 was synthesized in the Berlin lab[22] and the sample of HOAB was obtained commercially from Merck (Licristal, Art. No. 3102). Texture observations of planar and homeotropically aligned samples were carried out with Olympus BH-2 and Leitz Ortholux II POL-BK polarizing microscopes, the sample temperature regulated by Linkam or Instec hotstages. These setups were used also for electro-optic measurements on planar-aligned samples of 2.5 μm thickness (Chalmers MC2 assembly line, antiparallelly buffed polyimide alignment coating). Calorimetry investigations were carried out using Perkin-Elmer DSC 7 and Mettler Toledo DSCs. Dielectric spectroscopy measurements with simultaneous sample texture monitoring were carried out using HP 4192A and HP4294A bridges, a USB video camera (Logitech QuickCam Pro 4000) and DISCO measurement software (FLC Electronics) on 23.5 μm planar-aligned samples.

The optical tilt angle was measured using a technique first proposed by Bahr and Heppke[23] and refined by Giesselmann and co-workers,[24] where the optical transmission *T* of both states during saturated square wave switching was measured for several consecutive sample orientations φ. By fitting $\sin^2 \varphi$ functions to the two resulting $T(\varphi)$ data sets the tilt angle is extracted from their relative phase shift. The spontaneous polarization was measured by integrating the polarization reversal current while switching the sample with a triangular wave form electric field.[25]

Small-angle x ray scattering experiments were carried out on samples filled into Mark capillary tubes of 0.7 mm diameter. CuK_α radiation, a Kratky Compact camera, and an M. Braun 1D detector were used. A multiple Lorentz peak function was fitted to the scattering profile in order to get not only the layer thickness d but also the first- and second-order scattering intensities, needed for estimating the degree of smectic order. In order to get reasonable conformations of the mesogens and their respective lengths, the molecule structures were geometry optimized using MOPAC/AM1.

III. RESULTS AND DISCUSSION

A. The phase sequences of the different mixtures

In the phase diagram in Fig. 3(a) we see that we can distinguish four main regimes as the amount of (S,S)-M7BBM7 is increased. Initially the main effect of the AFLC is simply to chiralize the N and SmC phases of HOAB, but an increase in stability of the smectic phase at the cost of the nematic is also easy to recognize. At $x \approx 0.1$ a drastic change is seen: the SmC* phase is now followed by a narrow temperature range of SmA*, replaced by a TGB* phase (probably TGB$^*_A$) on further heating, and between N* and the isotropic phase blue phases (at least BP$^*_I$ and BP$^*_{III}$) are stable over a small temperature range. Characteristic texture examples are shown in Fig. 4.

With slightly more (S,S))-M7BBM7 the nematic phase disappears completely and SmA* is now the first liquid crystalline phase to form on cooling from the isotropic liquid. The blue and TGB* phases are only observed at the border between the N$^{(*)}$ regime and the A*-C* regime. These phases are generally attributed to exceptionally strong chiral influence, but in this case they appear in a mixture where nine out of ten molecules are nonchiral and the SmC* phase still has very long pitch (much longer than visible light wavelengths), so it seems unlikely that the chiral interactions would be particularly strong in this mixture. Rather, the position of the induced TGB* phase at the borderline between N* and SmA* in the phase diagram suggests that we can attribute its appearance to the frustration between the incompatible molecule organizations of cholesteric and smectic phases. As for the blue phases, their appearance may possibly also be understood as a frustration effect at the borderline between direct isotropic-N* and isotropic-SmA* transitions. One must of course take into consideration that S,S-M7BBM7 has two stereogenic centers of equal kind, and that the density of identical stereogenic centers therefore is higher than in a corresponding mixture with a monostereogenic compound. We have therefore also investigated systems where S,S-M7BBM7 has been replaced with homologs where one of the chiral terminal chains have been replaced with an achiral chain. The preliminary investigations clearly show that at least the TGB* phase can still be generated at about the same low concentration of monostereogenic chiral mesogen. The full results of these investigations, which are still on-going, will be published elsewhere.

As we move within the A*-C* regime towards larger amount of AFLC mesogen the clearing point is pushed upwards and the melting point downwards, giving the mixtures

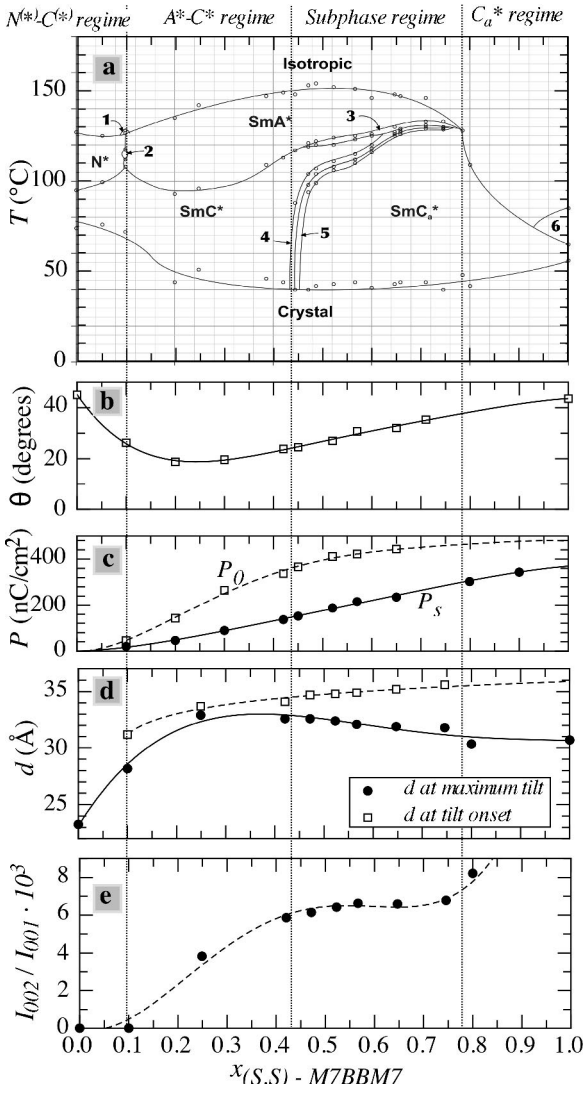

FIG. 3. Phase diagram (a), optical tilt angle θ (b), spontaneous polarization P_s and tilt-reduced polarization $P_0 = P_s/\sin\theta$ (c), layer spacing d (d) and smectic order estimate I_{002}/I_{001} (e), as functions of mixture composition, for the binary system HOAB/(S,S)-M7BBM7. The θ and P values have been obtained by fitting a power-law function to experimental data and extrapolating to $T_c - T = 50$ K, where T_c is the temperature of onset of tilt. In (a) the measured transition temperatures—indicated as rings—have been compiled from DSC, dielectric spectroscopy, and polarizing optical microscopy investigations. The following number coding has been used: 1-BP*, 2-TGB*, 3-SmC$^*_\alpha$, 4-SmC$^*_\beta$, 5-SmC$^*_\gamma$, 6-SmQ*. In (e) the values are averages over a range of ~20 K, well below the onset of smectic order.

a considerably larger mesophase range than either pure component. This raising of the clearing point and induction of a SmA* phase was also observed by Barretto *et al.*[26] when studying the effects of enantiomeric excess reduction in M7BBM7. The mixture containing all four stereoisomers in equal concentrations exhibited the highest clearing point and a 20 K broad SmA phase. Between this mixture and the pure (S,S)-isomer the system exhibited the unusual direct transition between the isotropic liquid and the SmC$^*_a$ phase.

As the amount of (S,S)-M7BBM7 is increased in the mixtures with HOAB, the SmA* phase range first rapidly increases at the cost of SmC* but from $x = 0.25-0.3$ this situation reverses. At $x \approx 0.44$ a new regime starts, namely, that of the chiral smectic-C subphases. The SmC$^*_\beta$ phase is the

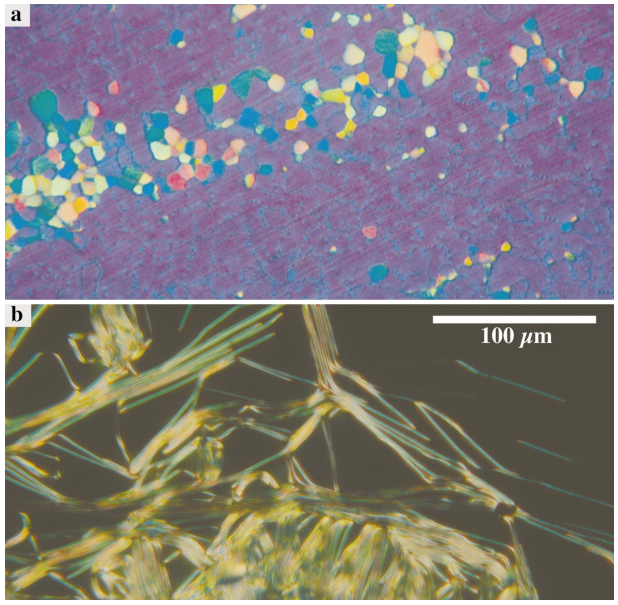

FIG. 4. (Color) The characteristic platelet texture of BP_I^* (a) and filament texture of the TGB^* phase growing into the homeotropic SmA^* background (b). The mixture has an (S,S)-M7BBM7 concentration $x=0.1$ and it is kept in a 5 μm planar-aligning cell (a) and between untreated glass plates (b).

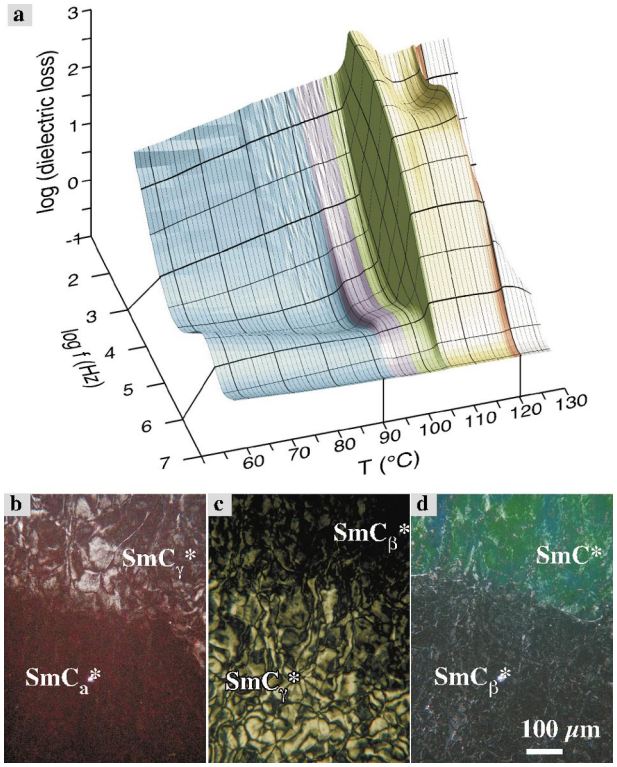

FIG. 5. (Color) (a) Dielectric spectrum of the $x=0.47$ mixture. Color coding: SmC_a^*—blue, SmC_γ^*—purple, SmC_β^*—green, SmC^*—yellow, SmC_α^*—orange, SmA^*—gray. Lower part: homeotropic textures at the SmC_a^*-SmC_γ^* (b), SmC_γ^*-SmC_β^* (c), and SmC_β^*-SmC^* (d) transitions. The two subphases are easily distinguished by their characteristic long-pitch schlieren textures from the SmC_a^* (dark red selective reflection color) and SmC^* (green) phases. Their strong similarity in (a) is unusual and probably a result of phase coexistence (see text).

first to appear, and it does so with an impressive temperature range of about 50 K, extending down to crystallization. With slightly more (S,S)-M7BBM7 the SmC_γ^* and then the SmC_a^* phase appear, the latter dominating the phase sequence as x increases further. SmC_β^* and SmC_γ^* now have temperature ranges more typical of these phases. In the $x=0.47$ mixture all three subphases, as well as SmC^* (separating SmC_α^* from SmC_β^*) and SmC_a^* could be distinguished by a combination of texture studies and dielectric spectroscopy measurements, cf. Fig. 5. Surprisingly, the SmC_β^* and SmC_γ^* phases gave almost identical dielectric response, an observation we will return to (and explain) below. The two phases could however be distinguished by means of texture studies, in particular in contact samples with well-characterized reference substances exhibiting the complete AFLC phase sequence. The anomalous low-frequency absorption at low temperatures of SmC^* is not a sign of a new phase but a result of memory effects appearing after the SmC_β^*-SmC^* transition.[27] The low-frequency increase in absorption is due to ionic conductivity and the tail at high frequencies results from the sample cell cutoff.[28]

Between $x=0.75$ and $x=0.8$ the subphases as well as SmA^* disappear from the phase sequence, leaving also the S,S-M7BBM7+HOAB mixture system with a direct isotropic-SmC_a^* transition. The work of Barretto and co-workers[26] concerned the high-temperature side of this transition and thus only the isotropic phase was carefully studied in that work. However, also the SmC_a^* phase below this transition is somewhat unusual, developing quite peculiar textures. Between untreated glass plates [Fig. 6(a)], the SmC_a^* phase first forms in homeotropic alignment as recognized as brightly colored (selective reflection) spots on the black isotropic background. On further cooling the edges of each spot turn planar as reflected in a bright yellow "corona" around many of the spots. If the mixture is filled into a polyimide-coated and electrode-equipped cell, planar alignment can be achieved by cooling from the isotropic phase with an electric field (b). We were not, however, able to achieve a uniform alignment of the layer normal, as seen in (c) where the SmC_a^* phase at slightly lower temperature is subjected to an electric field just at the threshold for switching the phase into the ferroelectric state. As this step of the switching process always spreads much faster along than across the layers (it is often referred to as "fingerlike switching"[29] because of this characteristic) it provides an excellent means of visualizing the smectic layer geometry. In most SmC_a^* phases, the ferroelectric state appears along concentric rings, reflecting the fact that the smectic layers usually form Dupin cyclides at the transition from isotropic to smectic.[30] In our case we noticed that the switching instead took place along left- and right-handed spiral-like paths in many places, possibly suggesting a somewhat different layer formation geometry at the direct isotropic-SmC_a^* transition.

When the SmC_a^* phase enters the phase sequence at $x \approx 0.46$, it does not appear at temperatures below those where SmC^* was stable in the A^*-C^* regime mixtures, but it more or less takes over that temperature range. The range of tilted smectic organization continuously increases slightly, diminishing the temperature range of SmA^*, but this does not save the SmC^* phase which disappears from the phase sequence at $x \approx 0.63$. The transition from SmC^* to SmC_a^*, via the subphases, is thus a transition which basically occurs horizon-

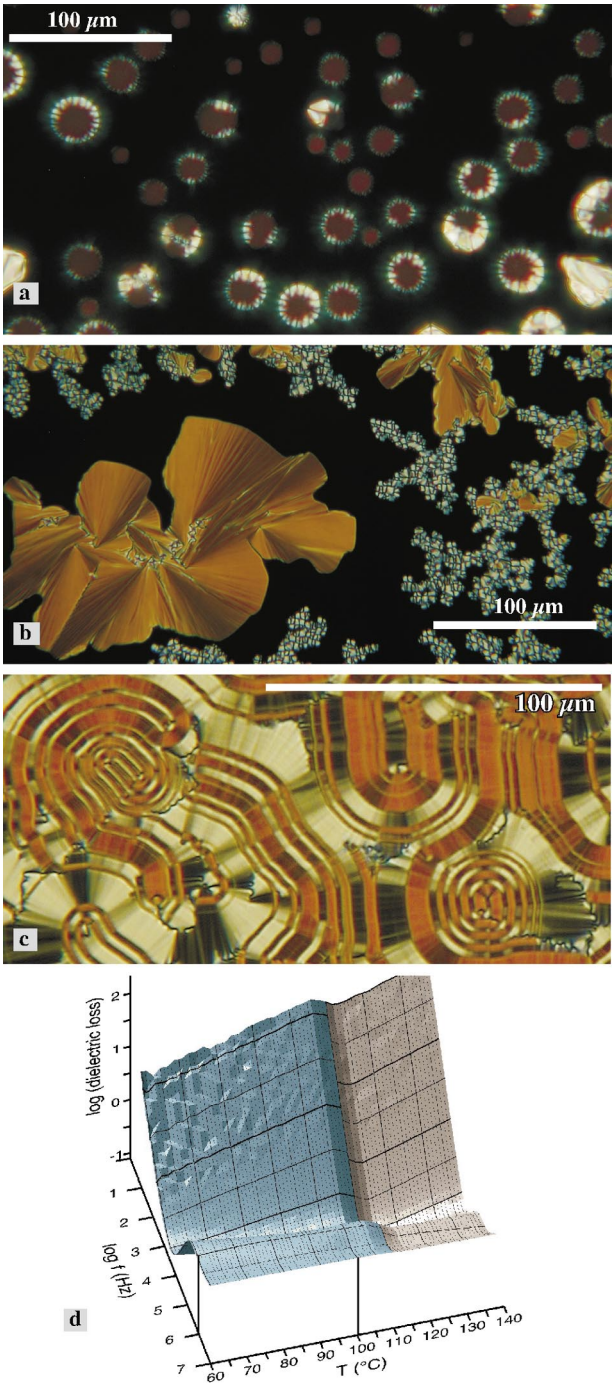

FIG. 6. (Color) Polarization microscopy textures of the direct transition from isotropic liquid to SmC_a^* of the $x=0.8$ mixture between untreated glass plates (a) and in a 2.5 μm polyimide-coated cell with an electric field (100 Hz square wave, 100 V_{pp}) applied to achieve planar alignment (b). In (c) the sample has been cooled as in (b) until the whole active area is SmC_a^*, and then a 100 Hz square wave electric field is applied at the threshold of switching from the antiferroelectric to ferroelectric state (22 V_{pp}). The dielectric absorption spectrum, measured on heating the planar-aligned 2.5 μm sample, is shown in (d), with SmC_a^* plotted in blue and isotropic in gray.

tally, i.e., the main driving variable is the mixture composition, not the temperature. In terms of general degree of order, all chiral smectic-C-type phases are thus on a very similar footage, a fact which is also demonstrated by the very small transition enthalpies between the phases, in the case that they follow one another on changing the temperature of a single

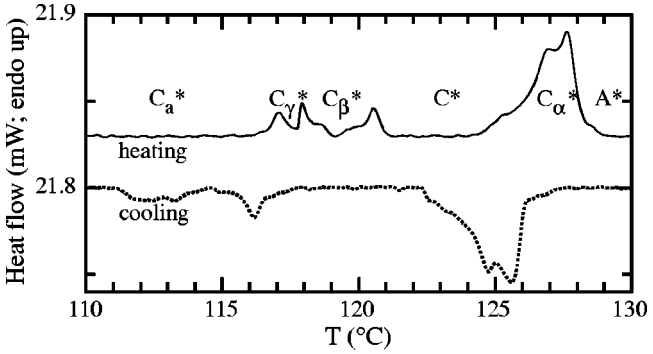

FIG. 7. DSC thermograms on heating (upper curve) and on cooling (lower dotted curve) of the $x=0.6$ mixture, obtained at 5 K/min scanning rate.

sample. We obtained DSC thermograms for seven different mixtures. In the vicinity of $x=0.5$, it was generally difficult to distinguish the transitions between the different smectic-C-type phases, a situation which is largely connected to strong coexistence between these phases (see below). At $x=0.6$, however, all transitions could be resolved on heating, as seen in the thermogram in Fig. 7. On cooling, many transitions were indistinguishable even in this mixture.

A striking characteristic of the (*S*,*S*)-M7BBM7+HOAB system is that in the vicinity of $x=0.5$ the tilted phases seem to coexist with one another in a quite extraordinary way. In Fig. 8 the texture of the $x=0.57$ mixture at 115 °C is shown. The picture looks as if it was taken while a temperature gradient was present across the sample, but this is not likely to be the case: decreasing the magnification one could see that the multiphase texture repeated itself back and forth in different directions, following an irregular pattern that could not have been created by a temperature gradient in the hot stage. This is most certainly not an example of phase coexistence in its strict definition, but rather a sign of spatial concentration variations resulting from a small degree of demixing. Its origin can be related to the nature of first-order transitions in mixtures, where phases of different composition coexist in biphasic regions. As we here have

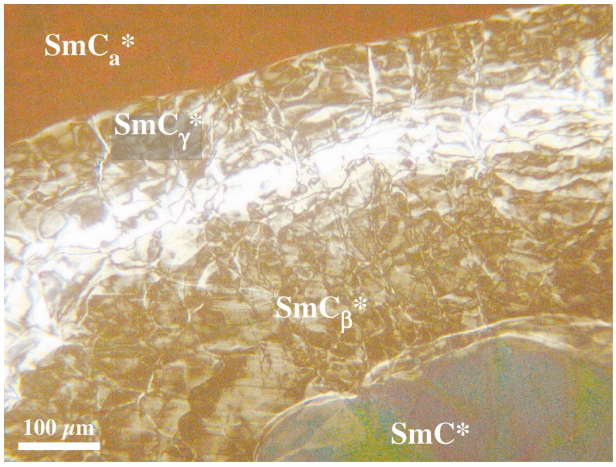

FIG. 8. (Color) The texture in an untreated microscope slide preparation with the $x=0.57$ mixture of (*S*,*S*)-M7BBM7 and HOAB at 115 °C. Note how, although there is essentially no temperature gradient across the sample, the SmC_a^*, SmC_β^*, SmC_γ^*, and SmC^* phases simultaneously exist next to one another.

four first-order transitions (three subphases in addition to SmC_a^* and SmC^*) very closely spaced in temperature, the situation that arises can be quite complex. Supporting this conclusion was the observation that the variations usually grew larger after the sample had been standing in the crystalline phase for some time (weeks to months), a state in which the miscibility of the two compounds is likely to be worse than in the liquid crystalline phases.

Considering how the phase sequence rapidly changes between $x=0.4$ and $x=0.6$, the spatial variations in transition temperatures observed in $x\approx 0.5$ mixtures become quite understandable. In this mixture range small changes in mixing ratio have considerable impact on the phase sequence of the system. Most conspicuously, a concentration variation of $\pm 2\%-3\%$ in an $x=0.45$ mixture shifts the system between a composition where the only tilted phase, down to crystallization, is SmC^* and one where this phase does not form below $\sim 100\,^\circ C$ and where the SmC_a^*, SmC_β^*, and SmC_γ^* phases instead form at the temperatures where the other system was SmC^*. In mixtures close to the borderline between FLC and AFLC behavior even a very small degree of concentration variation will thus dramatically affect the phase sequence. A consequence of the demixing tendency is that any measurement averaging over a large sample volume, such as a dielectric spectroscopy scan, may reflect a mixture of phases in the temperature range between SmC_a^* and SmC^*. This explains why the SmC_γ^* phase seemed to exhibit an unusually weak dielectric absorption, and why the SmC_β^* phase always exhibited a stronger absorption than in the ordinary antiferroelectric SmC_a^* phase, cf. the example from the $x=0.47$ mixture shown in Fig. 5. To verify that SmC_γ^* and SmC_β^* indeed both exist in this mixture, we had to carry out miscibility tests with reference AFLCs exhibiting both these phases.

B. The dependence of the SmC^* and SmC_a^* helical pitches on mixture composition

Since the absolute value of the helical pitch is not of prime interest to this work, but the trend of the pitch as a function of mixing ratio is all the more so, we only estimated the pitch by looking at the selective reflection colors in SmC^* and SmC_a^* in the mixtures where these phases appeared. In practice we monochromatized the light passing through the sample, set between crossed polarizers, with interference color filters, changing filter until maximum transmission was obtained.[31] This very simple method did not allow any pitch estimation for $x<0.35$, since the pitch was then too long to give selective reflection within the range covered by the set of interference filters.

Since the pitch depends not only on concentration of the chiral compound but also on temperature, we compared the minimum λ_r in each phase (SmC^* and SmC_a^*) between the different mixtures. The trend was the same in both phases: the inverse wavelength was found to depend roughly linearly on the mixing ratio, cf. Fig. 9. This suggests that the strength of chiral interactions increases linearly as more and more of the AFLC compound is added, as expected.

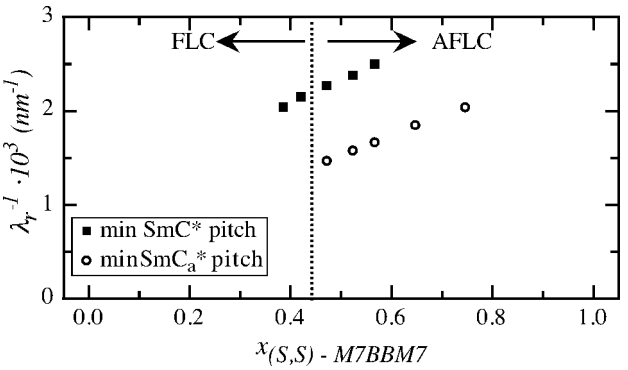

FIG. 9. Inverse estimated selective reflection wavelength λ_r^{-1} as a function of mixture composition.

C. Optical tilt angle, spontaneous polarization, and smectic layer characteristics

The tilt-angle reduced polarization $P_0=P_s/\sin\theta$—the second variable which gives a quantitative estimate of the strength of chiral interactions—varies monotonously as a function of mixing ratio, cf. Fig. 3(c). [The spontaneous polarization P_s depends as secondary order parameter on the primary order parameter θ, hence P_0 is a better "chirality measure" than P_s (Ref. 32).] In order to compare the different mixture compositions, a power-law function was fitted to the polarization data for each mixture and the result was used to obtain the polarization at $T_c-T=50$ K (by means of extrapolation when necessary, i.e., for mixtures which crystallized at higher temperatures), where it can be regarded as close to saturated. T_c is the temperature of onset of tilt.

The dependence of the optical director tilt angle θ on mixture composition [Fig. 3(b)] was somewhat more surprising. In both pure components θ is close to temperature independent and very high, about 45°, so one might expect an essentially composition-independent tilt angle. Instead θ at $T_c-T=50$ K exhibits a pronounced minimum at $x\approx 0.25$, a mixture composition which also produces the largest temperature range of SmA^*. This minimum in optical director tilt is accompanied by a minimum in actual molecule tilt, as evidenced by the low-temperature smectic layer spacing exhibiting a maximum at the same mixture composition [Fig. 3(d)]. This behavior suggests that the conflict created by mixing a compound which develops only synclinic SmC with one that prefers anticlinic organization suppresses the magnitude of tilt in general. If the tilt were diminished to zero, the conflict would be resolved, but since this does not happen in this system (possibly related to the fact that both components have a very strong tendency for tilt), we instead see the appearance of the SmC_β^* and SmC_γ^* phases, mediating between synclinicity and anticlinicity.

As mentioned in Sec. I, the smectic order parameter plays a central role in the study of different chiral smectic-C-type phases. The intensity of the $(00n)$ x ray scattering peak can be written as[33]

$$I_{00n} = \tau_n^2 I_{00n}^P, \tag{1}$$

where τ_n is the nth smectic order parameter, i.e., basically the nth coefficient in the Fourier expansion of the electron den-

sity modulation along the smectic layer normal (the exact Fourier coefficients are slightly rescaled from the corresponding order parameters), and I_{00n}^{P} is the intensity that the nth peak would have had in case of perfect smectic order. A perfectly sinusoidal electron density modulation, i.e., the extreme in unsharp smectic layer boundaries, has all order parameters with $n>1$ equal to zero, so in this case only the first-order diffraction peak is seen in the x ray data. As we are interested in quantifying the sharpness of the layer boundaries, i.e., the deviation from a sinusoidal electron density modulation, we would like to have a measure of τ_n.

In order to avoid the need for absolute intensities I_{00n} one often instead chooses to use the ratio between the second and first smectic order parameters as a measure of the layer boundary sharpness, since this is related to the relative intensities of the first- and second-order peaks through[33]

$$\left(\frac{\tau_2}{\tau_1}\right)^2 = \left(\frac{I_{002}}{I_{001}}\right)\left(\frac{I_{001}^{P}}{I_{002}^{P}}\right). \tag{2}$$

Whereas the intensities I_{001} and I_{002} are readily available from fitting, e.g., a multiple Lorentz peak function to the x ray scattering data, the intensities for the hypothetical perfectly ordered smectic state I_{001}^{P} and I_{002}^{P} are difficult to access. These parameters are related to the structure factors F_n of the phase along the smectic layer normal:

$$I_{00n}^{P} = |F_n|^2. \tag{3}$$

In principle, the structure factors can be calculated for each mesogenic structure by means of molecular modeling, but the result is strictly valid only for the particular conformation that has been chosen for the calculations. In the real system there will be considerable fluctuations around the most probable conformations, which do not necessarily comprise the one obtained through molecular modeling (which is done for individual molecules, i.e., gas phase). Next, the imperfect orientational order of the smectic phase must be taken into account. Additional complications arise from the mosaicity of the samples used and the possibility of multiple scattering. As we are studying mixtures, yet another problem is that it is far from obvious how to obtain an appropriate structure factor for each mixture composition. We have therefore settled with a study of the ratio I_{002}/I_{001} as the mixture composition is changed. Moreover, because the temperature variation of the order parameter was not of prime interest in this study we have averaged I_{002}/I_{001} over a temperature range of $\sim$20 K well below the onset of smectic order. This solution was chosen because of the rather low signal-to-noise ratio of the second-order peak, resulting in some scatter in the fitting results at each temperature. Since the temperature response of the smectic order parameter can be assumed to be saturated well below the transition into the smectic state, regardless of x, the data thus obtained are sufficient for obtaining the trend in smectic order as the mixture composition is varied. The result is shown in Fig. 3(e).

Although there is no maximum in I_{002}/I_{001} in the mixtures where the subphases are maximally stable, there is a distinct plateau in this region. Whereas the smectic order is constantly very low in the $N^{(*)}$-$C^{(*)}$ regime (no second-order peak was visible at all in these mixtures) and increases rapidly in the A^{*}-C^{*} regime, it is essentially constant in the subphase regime. Only when so much (S,S)-M7BBM7 has been added to the system that all liquid crystal phases but SmC_a^{*} have disappeared from the phase diagram do we see a tendency of further increase in the smectic order. More mixtures in the C_a^{*} regime would be necessary for drawing conclusions of the smectic order behavior at large x. From the available data we can however clearly conclude that the appearance of the subphases requires higher smectic order than what is necessary for the ordinary SmC^{*} phase, as expected.[4,18] But the degree of order seems to be the same as in ordinary AFLCs, exhibiting SmC_a^{*} below SmA^{*}, possibly with other types of chiral smectic-C phase in between.

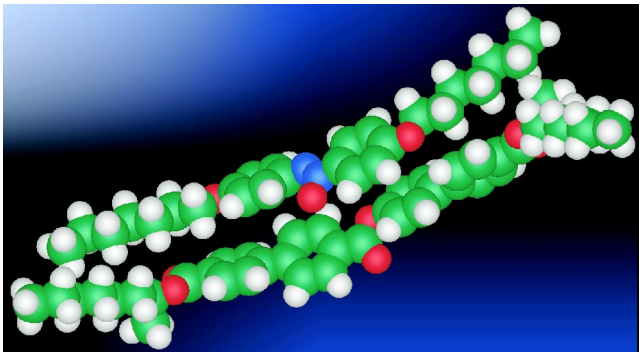

FIG. 10. A HOAB and (S,S)-M7BBM7 molecule pair as appearing after energy minimization using MOPAC/AM1.

The maximum in smectic layer spacing at $x\approx 0.25$ is quite unusual. The common behavior when mixing two smectogens with different layer spacing is that the layer spacing of the mixture shows a more or less linear dependence on the mixing ratio.[34] The strongly nonlinear behavior observed in our system resembles that reported by Diele and co-workers in a series of investigations on mixtures of swallow-tailed molecule liquid crystals with compounds having smaller rod-shaped molecules.[35] They explained the phenomenon using a concept they called "filled smectics" where the smaller molecules fill the free volume that is formed between the larger swallow-tailed molecules due to their bulky ends. A similar phenomenon may be responsible for the layer spacing behavior in our mixture system. Although the (S,S)-M7BBM7 molecule is not swallow tailed, the shorter HOAB molecule can pack quite well together with (S,S)-M7BBM7 in such a way that the effective length of the molecule pair is roughly the same as that of a single (S,S)-M7BBM7 molecule. The packing scheme resulting from MOPAC/AM1 energy optimization of a single (S,S)-M7BBM7-HOAB molecule pair is shown in Fig. 10. If the number of short molecules by large exceeds the number of long molecules, however, the overall packing can no longer be efficient in a smectic structure with large layer thickness, and this is why the layer thickness rapidly decreases if the amount of HOAB exceeds $\sim$75% of the mixture.

One should not understand this reasoning as if the molecules pair up two and two. The molecules of course constantly undergo thermally excited fluctuations in conforma-

tion as well as translations and rotations on a very fast time scale. On the other hand, it would be incorrect to treat the molecules as being completely independent of one another. Leadbetter introduced a coherence volume, with a size on the order of ten molecules, setting a microscopic limit below which one can expect some collective behavior in any liquid crystal phase.[36,37] The idea of molecular pair aggregation should be understood as some degree of correlated dynamics of neighboring HOAB and (S,S)-M7BBM7 molecules, promoted by certain combinations of conformations and relative positions leading to a particularly efficient packing, for instance as illustrated in Fig. 10.

IV. CONCLUSIONS

By mixing a mesogen forming nematic and smectic-C phases with one that forms the antiferroelectric SmC_a^* phase we create frustration on various levels. At the borderline between nematic and smectic organization, TGB^* and BP^* phases are induced, although the concentration of chiral mesogens is only $x \approx 0.1$, and at the border between synclinicity and anticlinicity the three chiral smectic-C subphases are induced. Furthermore, the untilted SmA^* phase, absent in both pure components, appears in the phase diagram over a broad range of intermediate mixture ratios. Its maximum temperature range is detected in the mixture ratio at which the SmC^* phase exhibits its minimum director tilt angle.

No simple correlation between any quantitative measure of chirality and the appearance of the subphases could be detected, although chirality is obviously a requirement for their formation, just as for TGB^* and BP^*. The degree of smectic order initially increases rapidly as (S,S)-M7BBM7 is added to HOAB, reaching a plateau in the mixture range where the subphases appear. The smectic order seems to increase again when the concentration of the AFLC mesogen is so high that the mixture exhibits a direct transition between the isotropic liquid and SmC_a^*.

ACKNOWLEDGMENTS

The authors thank V. Joeckel for helping them with the characterizations of the many mixtures. Financial support from the Alexander von Humboldt foundation (JPFL) and from the EU research program SAMPA (Synclinic and Anticlinic Mesophases for Photonics Applications) is gratefully acknowledged.

[1] R. B. Meyer, L. Liebert, L. Strzelecki, and P. Keller, J. Phys. (France) Lett. **36**, L69 (1975).
[2] E. Gorecka, D. Pociecha, M. Cepic, B. Zeks, and R. Dabrowski, Phys. Rev. E **65**, 061703 (2002).
[3] M. Cepic, E. Gorecka, D. Pociecha, B. Zeks, and H. Nguyen, J. Chem. Phys. **117**, 1817 (2002).
[4] J. P. F. Lagerwall, P. Rudquist, S. T. Lagerwall, and F. Giesselmann, Liq. Cryst. **30**, 399 (2003).
[5] J. P. F. Lagerwall, D. D. Parghi, D. Krüerke, F. Gouda, and P. Jägemalm, Liq. Cryst. **29**, 163 (2002).
[6] S. T. Lagerwall, *Ferroelectric and Antiferroelectric Liquid Crystals* (Wiley-VCH, Weinheim, 1999).
[7] L. S. Hirst, S. J. Watson, H. F. Gleeson *et al.*, Phys. Rev. E **65**, 041705 (2002).
[8] J. P. F. Lagerwall, Phys. Rev. E. (accepted).
[9] N. A. Clark and S. T. Lagerwall, Appl. Phys. Lett. **36**, 899 (1980).
[10] P. Mach, R. Pindak, A. M. Levelut *et al.*, Phys. Rev. E **60**, 6793 (1999).
[11] P. Mach, R. Pindak, A. M. Levelut, P. Barois, H. T. Nguyen, C. C. Huang, and L. Furenlid, Phys. Rev. Lett. **81**, 1015 (1998).
[12] M. Fukui, H. Orihara, Y. Yamada, N. Yamamoto, and Y. Ishibashi, Jpn. J. Appl. Phys., Part 2 **28**, L849 (1989).
[13] A. D. L. Chandani, Y. Ouchi, H. Takezoe, and A. Fukuda, Jpn. J. Appl. Phys., Part 2 **28**, L1261 (1989).
[14] E. Gorecka, A. D. L. Chandani, Y. Ouchi, H. Takezoe, and A. Fukuda, Jpn. J. Appl. Phys., Part 1 **29**, 131 (1990).
[15] T. Isozaki, T. Fujikawa, H. Takezoe, A. Fukuda, T. Hagiwara, Y. Suzuki, and I. Kawamura, Jpn. J. Appl. Phys., Part 2 **31**, L1435 (1992).
[16] A. Fukuda, Y. Takanishi, T. Isozaki, K. Ishikawa, and H. Takezoe, J. Mater. Chem. **4**, 997 (1994).
[17] K. Hiraoka, A. Taguchi, Y. Ouchi, H. Takezoe, and A. Fukuda, Jpn. J. Appl. Phys., Part 2 **29**, L103 (1990).
[18] Y. Takanishi, A. Ikeda, H. Takezoe, and A. Fukuda, Phys. Rev. E **51**, 400 (1995).
[19] D. Bennemann, G. Heppke, D. Lötzsch, and S. Paus, Presented at the 24th Arbeistagung Flüssigkristalle, Freiburg, Germany, 1995.
[20] D. Demus, H. Demus, and H. Zaschke, *Flüssige Kristalle in Tabellen* (Deutscher Verlag für Grundstoffindustrie, Leipzig, 1974), Vol. 1.
[21] C. Weygand and R. Gabler, J. Prakt. Chem. **155**, 332 (1940).
[22] D. Bennemann, G. Heppke, A. Levelut, and D. Lötzsch, Mol. Cryst. Liq. Cryst. Sci. Technol., Sect. A **260**, 351 (1995).
[23] C. Bahr and G. Heppke, Liq. Cryst. **2**, 825 (1987).
[24] F. Giesselmann, A. Langhoff, and P. Zugenmaier, Liq. Cryst. **23**, 927 (1997).
[25] K. Miyasato, S. Abe, H. Takezoe, and A. Fukuda, Jpn. J. Appl. Phys., Part 2 **22**, L661 (1983).
[26] G. Barretto, P. Collings, D. Bennemann, D. Lötzsch, and G. Heppke, Liq. Cryst. **28**, 629 (2001).
[27] J. P. F. Lagerwall, P. Rudquist, S. T. Lagerwall, and B. Stebler, Ferroelectrics **277**, 553 (2002).
[28] F. Gouda, K. Skarp, and S. T. Lagerwall, Ferroelectrics **113**, 165 (1991).
[29] J. F. Li, X. Y. Wang, E. Kangas, P. L. Taylor, C. Rosenblattt, Y. I. Suzuki, and P. E. Cladis, Phys. Rev. B **52**, R13075 (1995).
[30] A. J. Slaney, K. Takatoh, and J. W. Goodby, in *The Optics of Thermotropic Liquid Crystals*, edited by S. J. Elston and J. R. Sambles (Taylor & Francis, London, 1998), pp. 307–372.
[31] The light that is transmitted maximally between crossed polarizers, regardless of sample orientation, has the selective reflection wavelength λ_r, since the component which is not reflected is circularly polarized and thus passes through the analyzer.
[32] H. Stegemeyer, R. Meister, U. Hoffmann, A. Sprick, and A. Becker, J. Mater. Chem. **5**, 2183 (1995).
[33] J. Seddon, in *Handbook of Liquid Crystals*, edited by D. Demus, J. W. Goodby, G. Gray, H.-W. Spiess, and V. Vill (Wiley-VCH, 1998), Vol. 1, pp. 635–679.
[34] S. Diele, Ber. Bunsenges. Phys. Chem. **97**, 1326 (1993).
[35] S. Diele, G. Pelzl, W. Weissflog, and D. Demus, Liq. Cryst. **3**, 1047 (1988).
[36] A. J. Leadbetter and E. K. Norris, Mol. Phys. **38**, 669 (1979).
[37] A. Leadbetter and P. Wrighton, J. Phys. Colloq. **40**, 234 (1979).